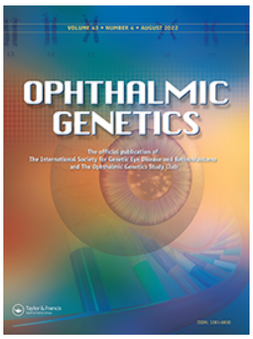

Ophthalmic Genetics

ISSN: (Print) (Online) Journal homepage: https://www.tandfonline.com/loi/iopg20

A novel phenotype associated with the R162W variant in the *KCNJ13* gene

Marion Schroeder, Virginie G. Peter, Lotta Gränse, Sten Andréasson, Carlo Rivolta & Ulrika Kjellström

To cite this article: Marion Schroeder, Virginie G. Peter, Lotta Gränse, Sten Andréasson, Carlo Rivolta & Ulrika Kjellström (2022) A novel phenotype associated with the R162W variant in the *KCNJ13* gene, Ophthalmic Genetics, 43:4, 500-507, DOI: 10.1080/13816810.2022.2068041

To link to this article: https://doi.org/10.1080/13816810.2022.2068041

Published online: 27 Apr 2022.

OPHTHALMIC GENETICS
2022, VOL. 43, NO. 4, 500–507
https://doi.org/10.1080/13816810.2022.2068041

Taylor & Francis
Taylor & Francis Group

RESEARCH REPORT

A novel phenotype associated with the R162W variant in the *KCNJ13* gene

Marion Schroeder[a], Virginie G. Peter[b,c], Lotta Gränse[a], Sten Andréasson[a], Carlo Rivolta[b,c], and Ulrika Kjellström[a]

[a]Department of Ophthalmology and Clinical Sciences Lund, Lund University, Skane University Hospital, Lund, Sweden; [b]Institute of Molecular and Clinical Ophthalmology Basel, Basel, Switzerland; [c]Department of Ophthalmology, University of Basel, Basel, Switzerland

ABSTRACT

Background: Pathogenic variants in *KCNJ13* have been associated with both autosomal dominant Snowflake vitreoretinal degeneration (SVD) and autosomal recessive Leber congenital amaurosis. SVD is characterized by aberrant vitreoretinal interface leading to increased risk of retinal detachment, crystalline retinal snowflake deposits, optic disc abnormalities, early-onset cataract, and cornea guttae. Reduced dark adaptation and reduced scotopic rod b-waves have also been described. We report a novel phenotype associated with the R162W variant in *KCNJ13*.

Methods: Four affected members of a Swedish family were included. Three of them were examined with best corrected visual acuity, Goldmann perimetry, full-field—and multifocal electroretinography, optical coherence tomography, fundus color photographs, fundus autofluorescence images, slit lamp inspection, and genetic testing. The fourth subject only managed genetic testing.

Results: All subjects carry the pathogenic missense variant; c.484C>T (NM_002242.4), R162W, in *KCNJ13*. ERG measurements revealed reduced macular—as well as general retinal function. Two of the subjects had a history of retinal detachment and the two younger subjects demonstrated early onset cataract. They all had structural macular changes and slightly gliotic optic discs.

Conclusion: In this family, the R162W variant in *KCNJ13*, previously described in association with SVD, causes a somewhat novel phenotype including macular dystrophy and moderate reduction of general retinal function as the main features combined with disc abnormalities, retinal detachment, and presenile cataract that has been described before. In times of up-coming gene-based therapies, it is important to report new genotype—phenotype associations to improve the possibilities to identify future treatment candidates.

ARTICLE HISTORY
Received January 20, 2022
Revised April 5, 2022
Accepted April 13, 2022

KEYWORDS
Cone-rod dystrophy; Snowflake vitreoretinal degeneration (SVD); *KCNJ13* variant; full-field electroretinography; multifocal electroretinography

Introduction

Inherited vitreoretinal degenerations include a broad spectrum of disorders associated with severe visual handicaps. Typically, these disorders show a complicated overlap concerning phenotype and genotype as well as mode of inheritance. Even though the knowledge of the molecular and genetic basis for vitreoretinal degenerations has evolved tremendously lately, many patients still have an ambiguous genotype, and it is therefore important to continuously describe new genotype—phenotype associations.

Pathological variants in the *KCNJ13* gene have been associated with both autosomal dominant (ad) Snowflake vitreoretinal degeneration (SVD) (1,2) and autosomal recessive (ar) Leber congenital amaurosis (LCA16) (3,4). SVD is characterized by congenital liquefaction of the vitreous with an abnormal vitreoretinal interface leading to increased traction on the retina and a risk of retinal detachment (1,5,6). Moreover, degenerative crystalline deposits, called snowflakes, can be found in the peripheral retina. Other features are abnormalities of the optic disc with absent cup, pallor or fibrosis, early-onset cataract, and cornea guttae (1,5,7). Concerning retinal function, reduced dark adaptation and a reduction of scotopic rod b-waves have been reported (5,6). Subjects with LCA16 often have congenital nystagmus. Poor night vision and reading difficulties at an early age are also typical and fundoscopy usually demonstrates an atypical pattern of rounded massive RPE pigmentations and macular RPE mottling as well as attenuated vessels (3,4). Full-field electroretinography (ffERG) shows no reliable rod—or cone responses (4).

The *KCNJ13* gene encodes an inwardly rectifying potassium channel, called Kir7.1 (4,8,9), that is located in the apical cell membrane of retinal pigment epithelium (RPE) cells (10–14). The Kir7.1 channel maintains the ion homeostasis in the subretinal space. Opening of the Kir7.1 channel facilitates potassium efflux from the RPE cells, thus counteracting the decrease in subretinal potassium level caused by light exposure (9,10,15,16). Defect or absent function of the Kir7.1 channel is suggested to result in excessive depolarization of RPE cells leading to Ca^{2+} overload and eventually cell death, explaining the association between the mutated dysfunctional channel and SVD and LCA16 (2,9,17).

Here, we describe a Swedish family in which the pathogenic *KCNJ13* variant; c.484C>T (p.Arg162Trp), R162W, segregate in an autosomal dominant manner, and is associated with a novel phenotype including macular dystrophy, moderate reduction of general cone—and rod function, early-onset cataract, slightly abnormal gliotic optic discs and retinal detachment.

CONTACT Ulrika Kjellström ulrika.kjellstrom@med.lu.se Department of Ophthalmology and Clinical Sciences Lund, Ögonkliniken Skånes Universitetssjukhus Lund, Kioskg 1, Lund 221 85, Sweden

Materials and methods

Subjects

This study includes four members from two generations of a Swedish family, presenting with a macular dystrophy displaying an autosomal dominant inheritance pattern. The proband, II:2, is a woman, that was aged 33, when she was referred to our clinic; the Department of Ophthalmology at Skåne University Hospital, a tertiary center for hereditary retinal disorders, due to previous macular hole, vitreoretinal traction and retinal detachment in her right eye and reduced visual acuity in her left eye. At her visit to the clinic, she told us that her father, I:1, and her elder sister, II:1, likewise suffer from severely reduced visual acuity in both eyes and therefore they were examined as well. Moreover, her paternal uncle, I:2, also has severely reduced visual acuity due to operations for retinal detachment. Unfortunately, he lives far away and was not healthy enough to manage the journey and all the ophthalmological tests, but he was able to provide a blood sample for DNA analysis. The study was conducted in accordance with the Tenets of the Declaration of Helsinki and it was approved by the Ethical Committee for Medical Research at Lund University and the Ethikkommission Nordwest- und Zentralschweiz (EKNZ). All subjects got a detailed written and oral explanation of the nature and possible consequences of the study and then gave their written consent for participation.

Control groups

To define the limits of normality for ffERG parameters in adults, a control group consisting of 24 healthy persons aged 30–67 years (mean 48) was used. Another group of 21 healthy individuals aged 30–64 (mean 46) was employed for multifocal ERG (mERG) data.

Ophthalmological examination

Best corrected visual acuity (BCVA) was tested monocularly on a decimal letter chart at 5 meters (m) and visual fields were mapped with a Goldmann perimeter, likewise monocularly, with standardized objects V4e, I4e, 04e, 03e, and 02e. Fundus color photographs and autofluorescence (FAF) images were captured with a Topcon DRI OCT Triton Plus (Topcon Corporation, 75–1, Hasunuma-cho, Itabashi-ku, Tokyo, Japan). The field of view was 45°±5%. For FAF images, Spaide filters with excitation wavelength 535–585 nm and barrier filters with wavelength 600–720 nm were used. Moreover, slit lamp—and fundus examinations were carried out.

Genetic analysis

DNA was extracted from venous blood drawn from the precubital vein in four affected individuals. The DNA of subject I:1 was sequenced using an Agilent SureSelect Human All Exon V6 kit (Agilent Technologies), by means of 150 bp (base-pair) paired-end sequencing on an Illumina NovaSeq 6000 S4 instrument. Raw sequence files were processed using an internal computational pipeline as described before, using the human genome sequence (build hg19/GRCh37) as a reference (18). Annotation of chr2: g.233633500G>A was verified by VariantValidator (19). Targeted sequencing of the identified variant in *KCNJ13* (NM_002242.4:c.484C>T) was performed in individuals I:1, II:1, and II:2 by means of Sanger sequencing under standard conditions. Additionally, the presence of this variant in all four individuals was confirmed by next-generation sequencing (NGS) using the Eye disease NGS panel of 288 genes at Asper Biogene (Asper Ophthalmics, Tartu, Estonia) https://www.asperbio.com/asper-ophthalmics/eye-diseases-ngs-panel-of-288-genes. Moreover, targeted NGS analysis of the *ABCA4* gene was performed in order to exclude the presence of potential deep intronic variants in the *ABCA4* gene.

Full-Field electroretinography

FfERGs were recorded with an Espion E^2 analysis system (Diagnosys, Lowell, Massachusetts, USA) according to the standardized guidelines for clinical electroretinography recommended by the International Society for Clinical Electrophysiology of Vision (ISCEV) (20). Measurements were obtained with a Burian-Allen bipolar corneal ERG contact lens electrode after 40 min of dark adaptation and with maximally dilated pupils (cyclopentolate 1% and 2.5% phenylephrine hydrochloride). The ground electrode was placed on the forehead. Responses were registered with a wide-band filter (−3 dB at 1 Hz and 500 Hz). Concerning ffERG curves, the a-wave amplitude, measured from the baseline to the bottom of the through, is considered to reflect photoreceptor activity (21,22) while the b-wave amplitude, measured from the bottom of the through to the top of the peak is considered to correspond to bipolar—and Müller cell activity (23–25) and also indirectly photoreceptor function. To ensure reproducibility, the recordings were repeated for all stimulus intensities until two successive equivalent curves were captured.

Multifocal electroretinography

MERGs were registered with a Visual Evoked Response Imaging System (VERIS Science 6; EDI, San Mateo, USA) using settings adhering to the ISCEV standards (20). A stimulus matrix consisting of 103 hexagons scaled with eccentricity to produce equal amplitudes of the responses all over the matrix was used. In the program, each hexagon independently alters between white and black according to a pseudorandom binary *m*-sequence at 75 Hz. Recordings were captured with a Burian-Allen bipolar ERG contact lens electrode with maximally dilated pupils (cyclopentolate 1% and 2.5% phenylephrine). Proper central fixation was monitored by an infrared (IR) eye camera mounted in the VERIS equipment enabling the investigator to continuously check the eye movements and fixation of the subject. The first-order component of the mERG was analyzed regarding amplitudes (A) and implicit times (IT) of P1 (first positive peak) within the five concentric rings (A 1–5 and IT 1–5) around the fovea. Ring 1, the innermost ring, represent the summed responses from the center and the first ring.

Table 1. Clinical features of the subjects.

Patient	Age	Gender	BVCA (RE, LE)	Goldmann perimetry	Vitreous changes	Retinal detachment	Presenile cataract	Hearing loss	Facial hypoplasia	Arthro-pathy
I:1	69	M	0.3, 0.3	LE cannot detect 02e	no	no	operated at unknown age	no	no	no
I:2	82	M	NM	NM	NK	yes	NK	no	NK	NK
II:1	43	F	0.08, 0.07	RE & LE paracentral scotoma inf+nas for I4e and 04e	no	no	yes	no	no	no
II:2	33	F	0.08, 0.5	RE inf +nas constriction	yes	yes	yes	no	no	no

BCVA = best-corrected visual acuity on a letter chart at 5 meters, RE = right eye, LE = left eye, M =male, F=female, NM=not measured, NK=not known, inf=inferior, nas=nasal.

Optical coherence tomography

A swept source OCT with a 1050 nm light source; Topcon DRI OCT Triton Plus (Topcon Corporation, 75–1, Hasunuma-cho, Itabashi-ku, Tokyo, Japan) was used to capture OCT b-scans with scan size 6 × 6 mm and scan density 512 × 128 in subjects that were examined awake (I:1, II:1 and III:2). The internal fixation target (pre-set for macular imaging) was applied. Cross sectional macular morphology was studied on B-scan images. Macular thickness, from the retinal pigment epithelium (RPE) to the inner limiting membrane (ILM), was noticed using the standard retinal thickness map of the OCT software.

Statistics

FfERG—and mERG amplitudes in subjects were considered significantly reduced if lower than the mean of the control group −1SD. Likewise, ffERG 30 Hz flicker implicit time was considered significantly delayed if exceeding the mean +1SD.

Results

DNA sequencing demonstrated the presence of a pathogenic missense variant, NM_002242.4:c.484C>T, p.(Arg162Trp), R162W, in exon 3/3 of the *KCNJ13* gene in both sisters as well as in their father and their uncle. All affected individuals were heterozygous for this variant. The c.484C>T substitution results in an arginine-to-tryptophan amino acid change that leads to the assembly of a non-functional potassium Kir7.1 channel producing a nonselective cation current that depolarizes cells in an incorrect way (1,2,4,17). It was previously demonstrated that the mutant subunit acts via a dominant negative effect (2,9). Genome-wide sequencing did not identify any other pathogenic variants in genes associated with retinal—or vitreoretinal degenerations. Nor did the additional NGS analysis of targeted regions of the *ABCA4* gene identify any deep intronic variants in the *ABCA4* gene.

The proband (II:2) has had slightly subnormal visual acuity since childhood. At the age of 32, one year before the referral to our clinic, she was diagnosed with a right eye macular hole, which was planned for surgery. Unfortunately, she developed a retinal detachment in the same eye and had to be operated for this instead. After the operation, BCVA was 0.08 in the right eye and 0.5 in the left eye (Table 1.) Goldmann perimetry turned out normal in the left eye, but in the operated right eye, all isopters (V4e, I4e, 03e and 02e) were constricted inferonasally. FfERG revealed slightly reduced amplitude and delayed IT for the 30 Hz flicker cone response (Table 2). Macular function was even more affected with reduced amplitudes in all rings of the mERG (Figure 1 and Table 2). Fundus examination (Table 3

Table 2. Electroretinographic findings for the subjects as well as the means and SDs for the control group. For amplitudes, the mean - 1SD is considered the lower limit of normality (the numbers within the brackets). Parameters below this are considered pathological and are highlighted in italics. For the implicit time (IT), the mean + 1SD is considered the upper limit of normality and values exceeding this is considered pathological and highlighted in italics. Measurements from the left eyes are shown since subject II:2 had had retinal detachment in her right eye. In subject I:1 though, mERG was registered only in the right eye and therefore right eye mERG values are included in the table for him.

Electrophysiological parameter	I:1	II:1	II:2	Control subjects
ffERG DA rod response Ampl (μV)	*124*	*147*	241	243±66 (177)
ffERG DA combined rod-cone response a-wave Ampl (μV)	*124*	*130*	236	190±45 (145)
ffERG DA combined rod-cone response b-wave Ampl (μV)	*231*	*249*	425	342±81 (261)
ffERG 30 Hz flicker cone response Ampl (μV)	*44*	*29*	*55*	77±18 (59)
ffERG 30 Hz flicker cone response IT (ms)	*39.0*	*38.5*	*36.5*	28,4±1,5 (29.9)
mERG Ring 1 Ampl (μV/deg2)	*25*	*10*	*22*	44±12 (32)
mERG Ring 2 Ampl (μV/deg2)	*21*	*9*	*16*	31±8 (23)
mERG Ring 3 Ampl (μV/deg2)	*20*	*7*	*13*	26±6 (20)
mERG Ring 4 Ampl (μV/deg2)	20	*9*	*11*	23±6 (17)
mERG Ring 5 Ampl (μV/deg2)	23	*9*	*11*	22±6 (16)

ffERG = full-field electroretinography, DA = dark adapted, Ampl = amplitude, Hz = Hertz, IT = implicit time, mERG = multifocal electrophysiology

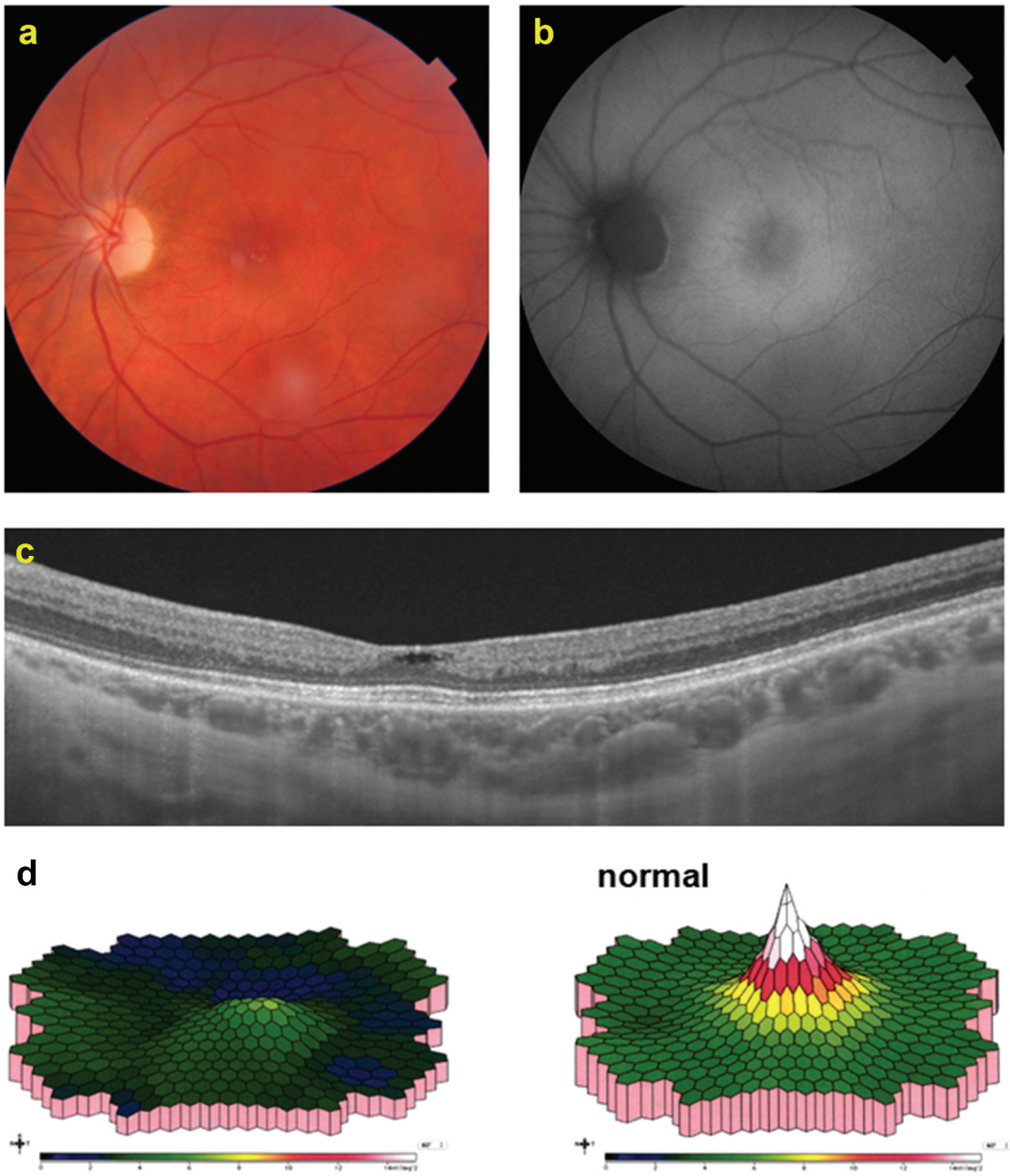

Figure 1. Clinical phenotype. Images of the left eye of the patient II:2 as described in detail in Table 3. A: Color fundus photograph displays a yellowish paracentral ring at the posterior pole. B: Fundus autofluorescence (FAF) image shows a corresponding paracentral ring with increased FAF in the posterior pole. C: OCT B-scan of the central macula reveals a lacunar substance loss in the inner retina and an increased hyperreflective band of the interdigitation zone subfoveally in the outer retina. D: Multifocal electrophysiology density plot showing reduced macular function.

and Figure 1) showed slightly pale optic discs on the temporal sides, and superionasally they were somewhat gliotic. In the maculae, discrete pigmentary changes were found, and subtle vitreous changes were also encountered. There were lacunar retinal substance losses in the fovea on OCT B-scans (Table 3 and Figure 1) and in the right macula the ellipsoid zone was absent, probably as a result of the previous macular hole. Moreover, OCT macular map revealed attenuation in all segments of both eyes. FAF images demonstrated small foci of reduced autofluorescence in the right eye and a paracentral ring of fine granular increase of autofluorescence around the fovea in the posterior pole of both eyes (Table 3 and Figure 1). Concerning general health, subject II:2 did not have any complaints (Table 1).

II:1, the elder sister of the proband, was diagnosed with hyperopia at the age of four and therefore was prescribed spectacles. Despite full-time glasses, vision did not improve and at the age of eight, Stargardt disease was suggested due to macular changes. The childhood examinations were performed in another clinic and therefore, we do not have access to the medical records from these visits. As far as we know, no genetic testing was carried out. At the visit to our department, BCVA was severely reduced to 0.08 in the right eye and 0.07 in the left eye (Table 1) and paracentral scotomas for I4e (15°) and 04e (10°) were outlined inferonasally on Goldmann perimetry. The amplitudes for all ffERG responses were slightly reduced, and the 30 Hz flicker cone IT was delayed (Table 2). Moreover, macular

Table 3. Description of optical coherence tomography (OCT), fundus autofluorescence (FAF) images and color fundus photographs in the subjects.

Patient	Age	Gender	OCT	FAF	Color fundus photograph
I:1	69	M	**RE/LE**: General retinal thinning of the macula. Partial loss of the ellipsoid zone temporally. Subfoveally an increased hyperreflective band under the external limiting membrane and above the RPE. **RE**: Hyperreflective retinal changes under the external limiting membrane even nasally and temporally.	Not available	**RE/LE**: Posterior pole with small yellowish drusenlike lesions. Slight temporal pallor of the optic discs and superionasally subtle gliosis. **LE**: Naevus from optic disc to the nasal fovea
I:2	82	M	Not available	Not available	Not available
II:1	43	F	**RE/LE**: General retinal thinning of the macula. Hyperreflective intraretinal foci. Paracentrally hyperreflective retinal changes with backscattering. **RE**: Central and paracentral atrophy. **LE**: Indifferent and missing outer retinal layers.	**RE/LE**: Macula with generally decreased autofluorescence and partially/patchy absence of autofluorescene of the central macula.	**RE/LE**: Patchy pigmentations in the central macula. Slight temporal pallor of the optic discs and superionasally subtle gliosis.
II:2	33	F	**RE/LE**: General retinal thinning of the macula. **RE**: Central and paracentral loss of the ellipsoid zone as well as less differentiable inner and outer retina layers. Central macula with thickened hyperreflective band corresponding to RPE/Bruch´s membrane layer complex. Outer and inner retina with lacunar substance loss in the central fovea. **LE**: General macular thinning of the inner retina, ganglion cell layer and inner nuclear layer, and paracentrally of the outer nuclear layer. Inner retina lacunar substance loss in the central fovea. Central and paracentral increased hyperreflective band corresponding the interdigitation zone.	**RE/LE**: Paracentral ring with increased autofluorescence. **RE**: Centrally and paracentrally small spots with decreased autofluorescence.	**RE/LE**: Paracentral yellowish ring. Slight temporal pallor of the optic discs and superionasally subtle gliosis.

RE= right eye, LE= left eye, M= male, F= female, RPE= retinal pigment epithelium.

function was markedly decreased with reduction within all rings of the mERG corresponding to a total loss of the ellipsoid zone and central scarring on OCT B-scans as well as widespread attenuation on OCT macular maps (Tables 2, 3, and Figure 2). Fundus examination revealed extensive pigmentary changes in the posterior pole and marked dark pigmentary clumps in the central macula (Table 3 and Figure 2). FAF images showed rounded central areas totally devoid of autofluorescence corresponding to the pigmentations and generally decreased autofluorescence in the posterior pole (Table 3 and Figure 2). The optic discs were slightly pale on the temporal sides, and superionasally they were somewhat gliotic as in the younger sister; II:2 (Figure 2). The vitreous was unremarkable in both eyes, while symmetrical moderate cortical and nuclear cataract was encountered. Subject II:1 did not have any general health problems (Table 1).

The father, I:1, was much older, around 60 years of age, when he first noticed symmetrical, progressive visual decline. Quite a few years later, he was referred to our department for electrophysiological examinations due to macular changes. By then, BCVA was 0.3 in both eyes (Table 1). He was already operated for cataract in both eyes, but he did not remember how long ago so the exact timing is uncertain, and thus we cannot establish whether the cataracts were presenile or not. Goldmann visual fields were mainly normal, but he could not detect the 02e object in his left eye. FfERG showed slightly reduced amplitudes for all stimulations and the 30 Hz cone flicker IT was delayed (Table 2). Macular function was even more reduced with total lack of the central peak, and reduced amplitudes in the three innermost rings of the mERG (Table 2 and Figure 3). OCT B-scans demonstrated irregularities in the ellipsoid and interdigitation zones and attenuation in all segments on the macular map (Table 3 and Figure 3). Fundus examination revealed somewhat pale temporal delineation of the optic discs and the superior poles was discreetly gliotic. In the posterior pole and just outside the vascular arcades, subtle pigmentary and small drusen like changes were encountered. Moreover, there was a naevus in the left eye, reaching from the optic disc almost to the fovea and inferiorly to the lower vascular arcade (Table 3 and Figure 3). No vitreous changes were found, and he did not demonstrate any signs of facial skeletal abnormalities, hearing loss or problems with his joints (Table 1).

The paternal uncle of the two sisters, I:2, had a history of severely reduced visual function and retinal detachments. Unfortunately, he lives far away from our department and due to his age could not manage to come all the way for further evaluation, but he provided us with a blood sample that confirmed the pathogenic missense variant; c.484C>T (p.Arg162Trp), R162W in *KCNJ13*. The younger brother, I:1, told us about his medical history which was free of hearing problems, arthropathies, orofacial abnormalities or other shortcomings of general health.

Discussion

We report the clinical findings of four members in a Swedish family with a novel phenotype caused by the pathogenic missense variant; NM_002242.4:c.484C>T, p.(Arg162Trp), R162W, in exon 3 of the *KCNJ13* gene which, previously, has been described in association with ad SVD (1,2). This new ad phenotype is most typically characterized by marked reduction of macular function and abnormal macular morphology, but also of a moderate effect on general cone function reflected by reduced 30 Hz flicker amplitudes and delayed flicker ITs. In two of the

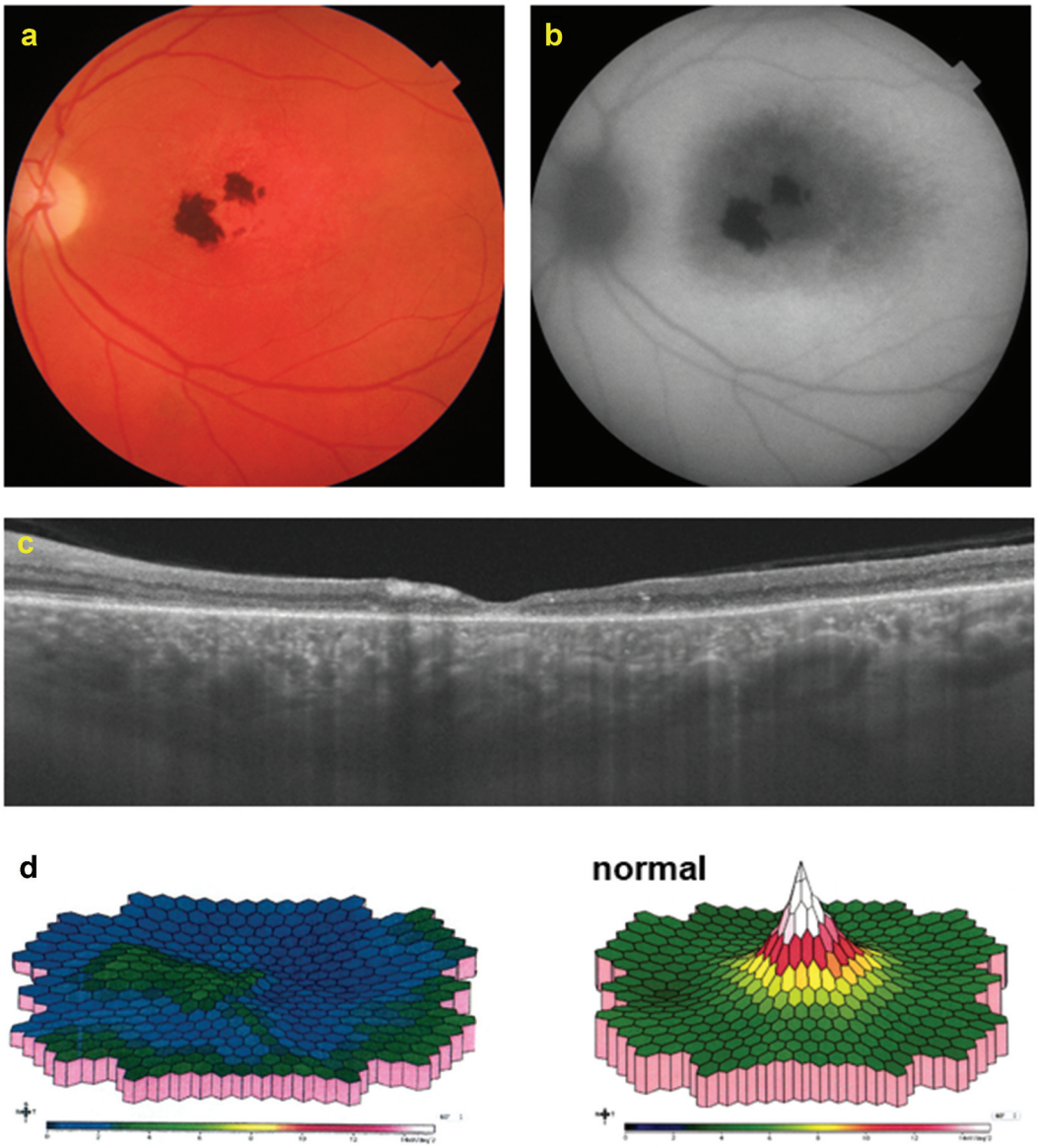

Figure 2. Clinical phenotype. Images of the left eye of the patient II:1 as described in detail in Table 3. A: Color fundus photograph shows central pigmentary changes. B: Fundus autofluorescence image presents overall decreased FAF at the posterior pole with partially loss of autofluorescence within. C: OCT B-scan shows central macular thinning mainly due to structural loss of the outer retinal layers, hyperreflective foci in the inner and outer retina and paracentral backscattering secondary to hyperreflective material in the inner retina. D: Multifocal electrophysiology density plot showing reduced macular function.

subjects, I:1 and II:1, also the isolated rod—and the combined rod—cone responses were affected. Previous studies on SVD have likewise described a reduction of rod function (5,6) but no macular dysfunction, which was the most prominent finding in our patients. In the youngest patient, II:2, the phenotype was somewhat less severe and more comparable to those from controls. Most likely this could be due to an age effect.

Moreover, SVD has been characterized by vitreous changes with abnormalities in the vitreoretinal interface leading to an increased risk of retinal detachment (1,5,6) and with degenerative peripheral retinal crystalline deposits (1,5,26). Two of our subjects, I:2 and II:2 had a history of retinal detachment but only one of the family members, II:1, displayed snowflake deposits (Figure 2). Other features that have been described in patients with SVD are abnormalities of the optic discs with pallor, fibrosis and absent cup, early-onset cataract, and cornea guttae (1,5,26). In line with this, all of our subjects had somewhat gliotic superior rims of the optic discs as well as temporal pallor and at least two of them; II:1 and II:2, had presenile cataract, while none of them demonstrated any corneal abnormalities. Neither did they display orofacial, auditory, skeletal, or joint abnormalities (Table 1) typical for Stickler syndrome (27–29), another disorder that is also associated with vitreoretinal changes. Thus, our patients demonstrate a phenotype that is novel in some perspectives; mainly concerning the primary macular—and general cone engagement, but also adheres to previous descriptions of SVD when it comes to the vitreous changes, retinal detachments, presenile cataracts and optic disc abnormalities. Another heterozygous *KCNJ13* variant; c.485 G>A (p.Arg162Gln), R162Q, which is associated with a change in the same amino acid as the c.848C>T has been described to cause still another phenotype with adult onset ad

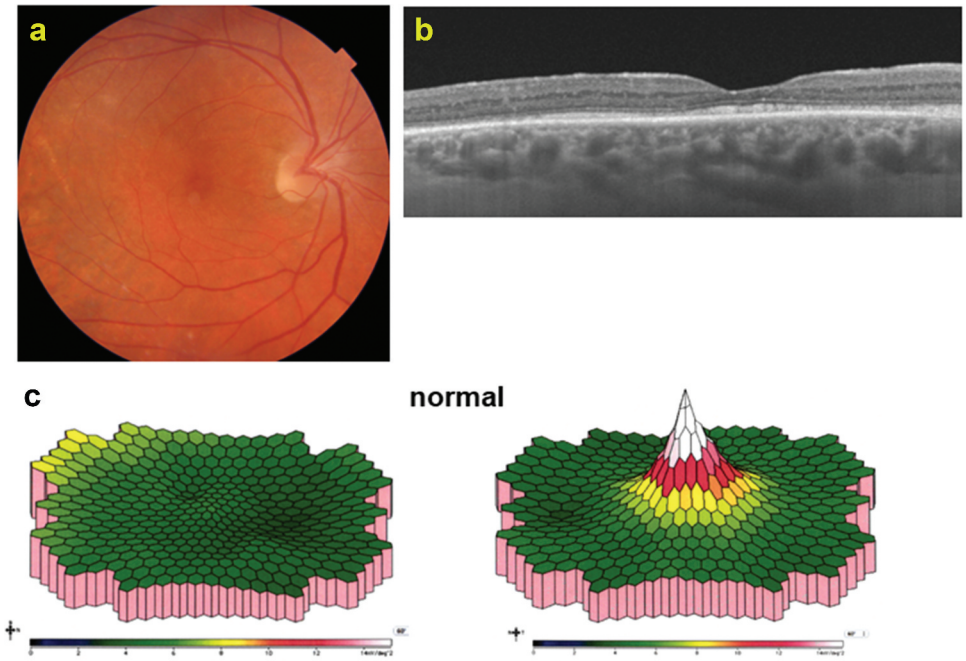

Figure 3. Clinical phenotype. Images of the right eye of the patient I:1 as described in detail in Table 3. A: Color fundus photograph shows yellowish drusenlike lesions in the posterior pole and beyond. B: OCT B-scan presents with paracentral and temporal loss of the ellipsoid zone and a subfoveally increased hyperreflective band between external limiting membrane and pigment epithelium. D: Multifocal electrophysiology density plot showing reduced macular function.

RP (4). The phenomenon with variants in the same gene leading to various phenotypes is quite common in retinal dystrophies (30) and makes correct diagnosing challenging.

In line with this, homozygous pathogenic variants in *KCNJ13* have also been described to cause ar LCA16 with severe and early onset visual handicap (3,4,7). In two of these studies (3,7), the parents of the probands were shown to be nonaffected, heterozygous *KCNJ13* carriers, while, in cases where the patients carry any of the variants c.848C>T (2,3), c.485 G>A, c.350A>G or c.827A>C (4) heterozygously they actually do have functional and structural ophthalmic alterations. An explanation for this could be that the latter variants result in a negative gain-of function with the mutant subunits exerting a dominant negative effect on the Kir7.1 channels (2,4,9) resulting in disrupted ion homeostasis in the subretinal space and by time cell death (2,9,17).

A drawback of our study is that it includes few patients. A larger material would, of course, have been eligible, but difficult to achieve for such a rare disease and we hope that our report anyway will contribute to valuable knowledge of *KCNJ13* associated disorders.

To conclude, our patients demonstrate a novel phenotype associated with the previously described pathogenic missense variant c.484C>T (p.Arg162Trp), R162W, in the *KCNJ13* gene and the phenotype is specified by macular dystrophy including severely reduced macular function and moderate decline of general retinal function as well as with early onset cataract, optic disc abnormalities and a risk of retinal detachment. In these days of increased hope for future gene-based therapies which are dependent on a correct genetic diagnosis, it is of even greater importance to report new genotype—phenotype associations to enable identification of treatment candidates.

Acknowledgements

We would like to thank Ing-Marie Holst and Boel Nilsson for skillful technical assistance.

Authors' contributions

All authors made substantial contributions to the design of the work, the acquisition, analysis and interpretation of data as well as drafting and revising of the content of the manuscript. All authors also approved the version to be published and take responsibility for all aspects of the work.

Consent for publication

All subjects gave their written consent to the publication of study results.

Consent to participate

All subjects got a detailed written and oral explanation of the nature and possible consequences of the study and then gave their written consent to participate.

Data availability statement

The authors have full control of all primary data and agree to allow the journal to review the data on request.

Ethical approvals

The study was conducted in accordance with the Tenets of the Declaration of Helsinki and it was approved by the Ethical Committee for Medical Research at Lund University and the Ethikkommission Nordwest- und Zentralschweiz (EKNZ).

Disclosure statement

No potential conflict of interest was reported by the author(s).

Funding

The work was supported by the Medical Faculty, Lund University, and grants from; Stiftelsen för synskadade i f.d. Malmöhus län; Stiftelsen Synfrämjandets Forskningsfond/Ögonfonden and the Swiss National Science Foundation [grant # 204285].

ORCID

Virginie G. Peter http://orcid.org/0000-0001-8157-9568
Carlo Rivolta http://orcid.org/0000-0002-0733-9950

References

1. Hejtmancik JF, Jiao X, Li A, Sergeev YV, Ding X, Sharma AK, Chan C-C, Medina I, Edwards AO. Mutations in KCNJ13 cause autosomal-dominant snowflake vitreoretinal degeneration. Am J Hum Genet. 2008;82(1):174–80. doi:10.1016/j.ajhg.2007.08.002. PMCID: PMC2253967.
2. Zhang W, Zhang X, Wang H, Sharma AK, Edwards AO, Hughes BA. Characterization of the R162W Kir7.1 mutation associated with snowflake vitreoretinopathy. Am J Physiol Cell Physiol. 2013;304(5):C440–9. doi:10.1152/ajpcell.00363.2012. PMCID: PMC3602648.
3. Pattnaik BR, Shahi PK, Marino MJ, Liu X, York N, Brar S, Chiang J, Pillers D-A-M, Traboulsi EI, et al. A novel KCNJ13 nonsense mutation and loss of Kir7.1 channel function causes leber congenital amaurosis (LCA16). Hum Mutat. 2015;36(7):720–27. doi:10.1002/humu.22807.
4. Sergouniotis PI, Davidson AE, Mackay DS, Li Z, Yang X, Plagnol V, Moore A, Webster A. Recessive mutations in KCNJ13, encoding an inwardly rectifying potassium channel subunit, cause leber congenital amaurosis. Am J Hum Genet. 2011;89(1):183–90. doi:10.1016/j.ajhg.2011.06.002. PMCID: PMC3135807.
5. Edwards AO. Clinical features of the congenital vitreoretinopathies. Eye. 2008;22(10):1233–42. doi:10.1038/eye.2008.38.
6. Hirose T, Wolf E, Schepens CL. Retinal functions in snowflake degeneration. Ann Ophthalmol. 1980;12(10):1135–46. Accession Number: 7283319.
7. Khan AO, Bergmann C, Neuhaus C, Bolz HJ. A distinct vitreo-retinal dystrophy with early-onset cataract from recessive KCNJ13 mutations. Ophthalmic Genet. 2015;36(1):79–84. doi:10.3109/13816810.2014.985846.
8. Derst C, Doring F, Preisig-Muller R, Daut J, Karschin A, Jeck N, Weber S, Engel H, Grzeschik K-H. Partial gene structure and assignment to chromosome 2q37 of the human inwardly rectifying K+ channel (Kir7.1) gene (KCNJ13). Genomics. 1998;54(3):560–63. doi:10.1006/geno.1998.5598.
9. Kumar M, Pattnaik BR. Focus on Kir7.1: physiology and channelopathy. Channels (Austin). 2014;8(6):488–95. doi:10.4161/19336950.2014.959809. PMCID: PMC4594557.
10. Hibino H, Inanobe A, Furutani K, Murakami S, Findlay I, Kurachi Y. Inwardly rectifying potassium channels: their structure, function, and physiological roles. Physiol Rev. 2010;90(1):291–366. doi:10.1152/physrev.00021.2009.
11. Ookata K, Tojo A, Suzuki Y, Nakamura N, Kimura K, Wilcox CS, Hirose S. Localization of inward rectifier potassium channel Kir7.1 in the basolateral membrane of distal nephron and collecting duct. J Am Soc Nephrol. 2000;11(11):1987–94. doi:10.1681/ASN.V11111987.
12. Yang D, Swaminathan A, Zhang X, Hughes BA. Expression of Kir7.1 and a novel Kir7.1 splice variant in native human retinal pigment epithelium. Exp Eye Res. 2008;86(1):81–91. doi:10.1016/j.exer.2007.09.011. PMCID: PMC2697662.
13. Yang D, Zhang X, Hughes BA. Expression of inwardly rectifying potassium channel subunits in native human retinal pigment epithelium. Exp Eye Res. 2008;87(3):176–83. doi:10.1016/j.exer.2008.05.010. PMCID: PMC2612002.
14. Yang J, Wang L, Song H, Sokolov M. Current understanding of usher syndrome type II. Front Biosci (Landmark Ed). 2012;17(1):1165–83. doi:10.2741/3979. PMCID: PMC3303697.
15. Doring F, Derst C, Wischmeyer E, Karschin C, Schneggenburger R, Daut J, Karschin A. The epithelial inward rectifier channel Kir7.1 displays unusual K+ permeation properties. J Neurosci. 1998;18(21):8625–36. doi:10.1523/JNEUROSCI.18-21-08625.1998. PMCID: PMC6793533.
16. Hughes BA, Takahira M. Inwardly rectifying K+ currents in isolated human retinal pigment epithelial cells. Invest Ophthalmol Visual Sci. 1996;37(6):1125–39.
17. Pattnaik BR, Tokarz S, Asuma MP, Schroeder T, Sharma A, Mitchell JC, Edwards AO, Pillers D-A-M. Snowflake vitreoretinal degeneration (SVD) mutation R162W provides new insights into Kir7.1 ion channel structure and function. PloS One. 2013;8(8):e71744. doi:10.1371/journal.pone.0071744. PMCID: PMC3747230.
18. Peter VG, Quinodoz M, Sadio S, Held S, Rodrigues M, Soares M, Sousa AB, Coutinho Santos L, Damme M, Rivolta C, et al. New clinical and molecular evidence linking mutations in ARSG to Usher syndrome type IV. Hum Mutat. 2021;42(3):261–71. doi:10.1002/humu.24150.
19. Freeman PJ, Hart RK, Gretton LJ, Brookes AJ, Dalgleish R. VariantValidator: accurate validation, mapping, and formatting of sequence variation descriptions. Hum Mutat. 2018;39(1):61–68. doi:10.1002/humu.23348. PMCID: PMC5765404.
20. Robson AG, Nilsson J, Li S, Jalali S, Fulton AB, Tormene AP, Holder GE, Brodie SE. ISCEV guide to visual electrodiagnostic procedures. Doc Ophthalmol. 2018;136(1):1–26. doi:10.1007/s10633-017-9621-y. PMCID: PMC5811581.
21. Brown KT, Watanabe K. Isolation and identification of a receptor potential from the pure cone fovea of the monkey retina. Nature. 1962;193(4819):958 passim. doi:10.1038/193958a0.
22. Penn RD, Hagins WA. Signal transmission along retinal rods and the origin of the electroretinographic a-wave. Nature. 1969;223(5202):201–04. doi:10.1038/223201a0.
23. Green DG, Kapousta-Bruneau NV. A dissection of the electroretinogram from the isolated rat retina with microelectrodes and drugs. Vis Neurosci. 1999;16(4):727–41. doi:10.1017/s0952523899164125.
24. Robson JG, Frishman LJ. Dissecting the dark-adapted electroretinogram. Doc Ophthalmol. 1998;95(3–4):187–215. doi:10.1023/a:1001891904176.
25. Tian N, Slaughter MM. Correlation of dynamic responses in the on bipolar neuron and the b-wave of the electroretinogram. Vision Res. 1995;35(10):1359–64. doi:10.1016/0042-6989(95)98715-L.
26. Lee MM, Ritter R 3rd, Hirose T, Vu CD, Edwards AO. Snowflake vitreoretinal degeneration: follow-up of the original family. Ophthalmology. 2003;110(12):2418–26. doi:10.1016/S0161-6420(03)00828-5.
27. Stickler GB, Hughes W, Houchin P. Clinical features of hereditary progressive arthro-ophthalmopathy (Stickler syndrome): a survey. Genet Med. 2001;3(3):192–96. doi:10.1097/00125817-200105000-00008.
28. Rose PS, Levy HP, Liberfarb RM, Davis J, Szymko-Bennett Y, Rubin BI, Tsilou E, Griffith AJ, Francomano CA. Stickler syndrome: clinical characteristics and diagnostic criteria. Am J Med Genet a. 2005;138A(3):199–207. doi:10.1002/ajmg.a.30955.
29. Robin NH, Moran RT, Ala-Kokko L. Stickler Syndrome. In: Adam M, Ardinger H, Pagon R, Wallace S, Bean L, and Stephens K, et al., editors. GeneReviews((R)). Seattle (WA); 1993; p. 1993–2022.
30. Berger W, Kloeckener-Gruissem B, Neidhardt J. The molecular basis of human retinal and vitreoretinal diseases. Prog Retin Eye Res. 2010;29(5):335–75. doi:10.1016/j.preteyeres.2010.03.004.